Scott A. Soleimanpour,[1] Alana M. Ferrari,[2] Jeffrey C. Raum,[2] David N. Groff,[2] Juxiang Yang,[2] Brett A. Kaufman,[3] and Doris A. Stoffers[2]

Diabetes Susceptibility Genes *Pdx1* and *Clec16a* Function in a Pathway Regulating Mitophagy in β-Cells

Diabetes 2015;64:3475–3484 | DOI: 10.2337/db15-0376

Mitophagy is a critical regulator of mitochondrial quality control and is necessary for elimination of dysfunctional mitochondria to maintain cellular respiration. Here, we report that the homeodomain transcription factor Pdx1, a gene associated with both type 2 diabetes and monogenic diabetes of the young, regulates mitophagy in pancreatic β-cells. Loss of Pdx1 leads to abnormal mitochondrial morphology and function as well as impaired mitochondrial turnover. High-throughput expression microarray and chromatin occupancy analyses reveal that Pdx1 regulates the expression of *Clec16a*, a type 1 diabetes gene and itself a key mediator of mitophagy through regulation of the E3 ubiquitin ligase Nrdp1. Indeed, expression of Clec16a and Nrdp1 are both reduced in Pdx1 haploinsufficient islets, and reduction of Pdx1 impairs fusion of autophagosomes containing mitochondria to lysosomes during mitophagy. Importantly, restoration of Clec16a expression after Pdx1 loss of function restores mitochondrial trafficking during mitophagy and improves mitochondrial respiration and glucose-stimulated insulin release. Thus, Pdx1 orchestrates nuclear control of mitochondrial function in part by controlling mitophagy through Clec16a. The novel Pdx1-Clec16a-Nrdp1 pathway we describe provides a genetic basis for the pathogenesis of mitochondrial dysfunction in multiple forms of diabetes that could be targeted for future therapies to improve β-cell function.

Pancreatic β-cells depend on mitochondrial respiration to generate the ATP required for glucose-stimulated insulin secretion (GSIS), which is required to maintain glucose homeostasis and is impaired in all forms of diabetes (1). Complex regulatory networks coordinate mitochondrial respiration, which depends on the maintenance of both mitochondrial mass and metabolic function. Mitochondrial autophagy or mitophagy is a quality-control mechanism that is necessary for the selective elimination of dysfunctional mitochondria to maintain cellular respiration (1).

Despite the importance of mitophagy to cellular function, direct transcriptional regulators of mitophagy have never been identified in mammalian cells. The helix-loop-helix transcription factor Rtg3, a regulator of the retrograde signaling pathway (RTG), is a transcriptional regulator of mitophagy in *Saccharomyces cerevisiae*; however, no conserved mammalian ortholog of Rtg3 has been identified (2). Pancreatic and duodenal homeobox (Pdx)1 is a homeodomain transcription factor associated with type 2 diabetes (T2D) and monogenic diabetes of the young (3,4). Pdx1 is a master regulator of pancreatic β-cell development and adult β-cell function and is vital for upstream control of insulin gene transcription, endoplasmic reticulum (ER) homeostasis, β-cell survival, and mitochondrial respiration (5–7). While Pdx1 deficiency has been associated with impaired mitochondrial function, the pathways by which Pdx1 controls mitochondrial metabolism have not fully been elucidated.

Here, we report that Pdx1 regulates mitochondrial function through its transcriptional control of mitophagy in pancreatic β-cells. Pdx1 directs autophagosome-lysosome fusion during mitophagy through transcriptional regulation of C-type lectin domain family 16, member A (*Clec16a*),

[1]Division of Metabolism, Endocrinology and Diabetes, Department of Internal Medicine, University of Michigan Medical School, Ann Arbor, MI
[2]Division of Endocrinology, Diabetes and Metabolism, Department of Medicine, Institute for Diabetes, Obesity and Metabolism of the University of Pennsylvania Perelman School of Medicine, Philadelphia, PA
[3]Division of Cardiology, Vascular Medicine Institute, Department of Medicine, University of Pittsburgh School of Medicine, Pittsburgh, PA

Corresponding authors: Scott A. Soleimanpour, ssol@med.umich.edu, and Doris A. Stoffers, stoffers@mail.med.upenn.edu.

Received 19 March 2015 and accepted 2 June 2015.

This article contains Supplementary Data online at http://diabetes.diabetesjournals.org/lookup/suppl/doi:10.2337/db15-0376/-/DC1.

a type 1 diabetes (T1D) gene that we recently found to be a mediator of mitophagy in pancreatic β-cells through its interaction with, and regulation of, the E3 ubiquitin ligase neuregulin receptor degradation protein (Nrdp)1 (8). Overexpression of Clec16a restores Nrdp1 expression and mitophagy and ameliorates defects in mitochondrial respiration and insulin secretion after Pdx1 deficiency.

RESEARCH DESIGN AND METHODS

Animals

Pdx1 heterozygous mice, *Pdx1*^{lacZko} (courtesy of Dr. Chris Wright, Vanderbilt University), and *Pdx1*^{tTA} (courtesy of Dr. Raymond MacDonald, University of Texas Southwestern Medical Center) were maintained on a C57BL/6 background and housed on a standard 12-h light/12-h dark cycle with ad libitum access to food and water. Similar results were observed between both *Pdx1* heterozygous mouse models and were used interchangeably for animal studies. All animal procedures were approved by the University of Pennsylvania Institutional Animal Care and Use Committee.

Oxygen Consumption Assays

Oxygen consumption was measured on isolated islets by a Clark-type O_2 electrode (Strathkelvin Instruments) or adherent cells using a XF24 Flux Analyzer (Seahorse Bioscience) as previously described (8).

Chromatin Immunoprecipitation

Chromatin isolated from three independent nondiabetic human islet donors (kindly provided by Dr. Ali Naji, University of Pennsylvania) was isolated and prepared as previously described (9). Immunoprecipitations were performed as previously described with anti-Pdx1 antiserum (253) (10). Chromatin immunoprecipitation (ChIP) PCR was performed with the following primers: *Clec16a* intron site 1 F, GAGTTCACAAGAGTGGCTTGG, and R, CCCACT CATTAATCACCTCCA; *Clec16a* intron site 2 F, TGGCAGCT GAGTAACTTAGGA, and R, CTTTTTGCCTTTTTGGATGG; *Pdx1* F, GTCCACACTTTAATTGGTTTACAGC, and R, CTCC CGAGCCATTTAACAG; *Albumin* F, GGAGTCCTGAGGGTA GCAGAAG, and R, ACCGGTCTCCCATTTTCCA.

Transmission Electron Microscopy

Pancreata were harvested from *Pdx1*$^{+/+}$ and *Pdx1*$^{+/-}$ littermates, minced into small pieces, and fixed with 2.5% glutaraldehyde and 2.0% paraformaldehyde (PFA) in 0.1 mol/L sodium cacodylate buffer, pH 7.4, overnight at 4°C and prepared as previously described (7). Images were collected at 80 KeV on a FEI Tecnai12 microscope equipped with a Gatan US1000 2 K CCD using Serial electron microscopy (EM) to montage regions of interest.

Analysis of Islet cDNA Microarrays

High-throughput gene expression profiling of islets (~12,000 targets in total) from *Pdx1*$^{+/+}$ and *Pdx1*$^{+/-}$ littermates was previously performed as described (7). Microarray results were filtered for overlap with the mouse MitoCarta database (11) supplemented with 51 additional autophagy/mitophagy targets, including ambra1, atg10, atg12, atg13, atg14, atg16, atg2, atg3, atg4, atg5, atg7, atg9, becn1, bif1, bnip3l, clec16a, fip200, fis1, gabarap, gabarapl2, gate-16, ip3r, kiaa0226, lamp2, map1lc3a, map1lc3b, mfn1, mfn2, mtor, naf1, opa1, p150, park2, pink1, rb1cc1, rnf41, rubicon, ulk1, ulk2, usp8, uvrag, vps11, vps16, vps18, vps33, vps34, vps39, wipi1, wipi2, wipi3, and wipi4. 871 of 1150 potential targets were identified on the previously performed microarrays (see all results in Supplementary Table 1). For statistical analysis of all microarray data, genes were called differentially expressed using the significance analysis of microarrays one class response package with a false discovery rate (FDR) of 20% (7).

Islet Isolation and Tissue Culture

Mouse islets were isolated after pancreatic duct cannulation and type IV collagenase digestion (Worthington). Islets were cultured in RPMI-1640 media with supplementation as previously described (12). Min6 mouse insulinoma cells were maintained in growth medium (DMEM including heat-inactivated FBS, penicillin/streptomycin, sodium pyruvate, and β-mercaptoethanol) as previously described (12).

Morphologic Analyses

Cells grown on Lab-Tek chamber slides (Nunc) were fixed with 4% PFA for 15 min at room temperature. For organelle staining assays, Min6 cells were treated with 100 nmol/L Mitotracker Deep Red FM or 50 nmol/L Lysotracker Red DND-99 (Molecular Probes) for 30 min prior to fixation. Analysis was performed with a spinning-disk confocal microscope (Perkin Elmer). Images were captured using an EM-CCD digital camera (Hamamatsu). Colocalization analysis of subcellular structures was performed using the JACoP ImageJ plugin (13). LC3 and LC3–green fluorescent protein (GFP) puncta were quantified and estimated using previously published guidelines (14).

Glucose and Insulin Measurements

Intraperitoneal glucose tolerance tests (2 g/kg D-glucose) were performed as previously described (9). Static incubation assays for insulin release were performed as previously described (15). Insulin concentrations were measured by ELISA (Crystal Chem).

Immunocytochemistry

After fixation and PBS washes, immunocytochemical staining was performed using the following antisera: rabbit anti-LC3 (MBL), rat anti-Lamp1 (1D4B; Developmental Studies Hybridoma Bank), mouse anti-Mfn2 (Abcam), and species-specific Cy2-, Cy3-, and Cy5-conjugated secondary antisera (Jackson Immunoresearch). Nuclear labeling was performed with DAPI (Molecular Probes).

Immunohistochemistry

Pancreata were fixed in 4% PFA, embedded in paraffin, and sectioned. Antisera were guinea pig anti-insulin (Dako), mouse anti-Mfn2 (Abcam), rabbit anti-LC3 (MBL), and species-specific Cy2-, Cy3-, and Cy5-conjugated secondary antisera (Jackson Immunoresearch). Nuclear labeling was performed with DAPI (Molecular Probes).

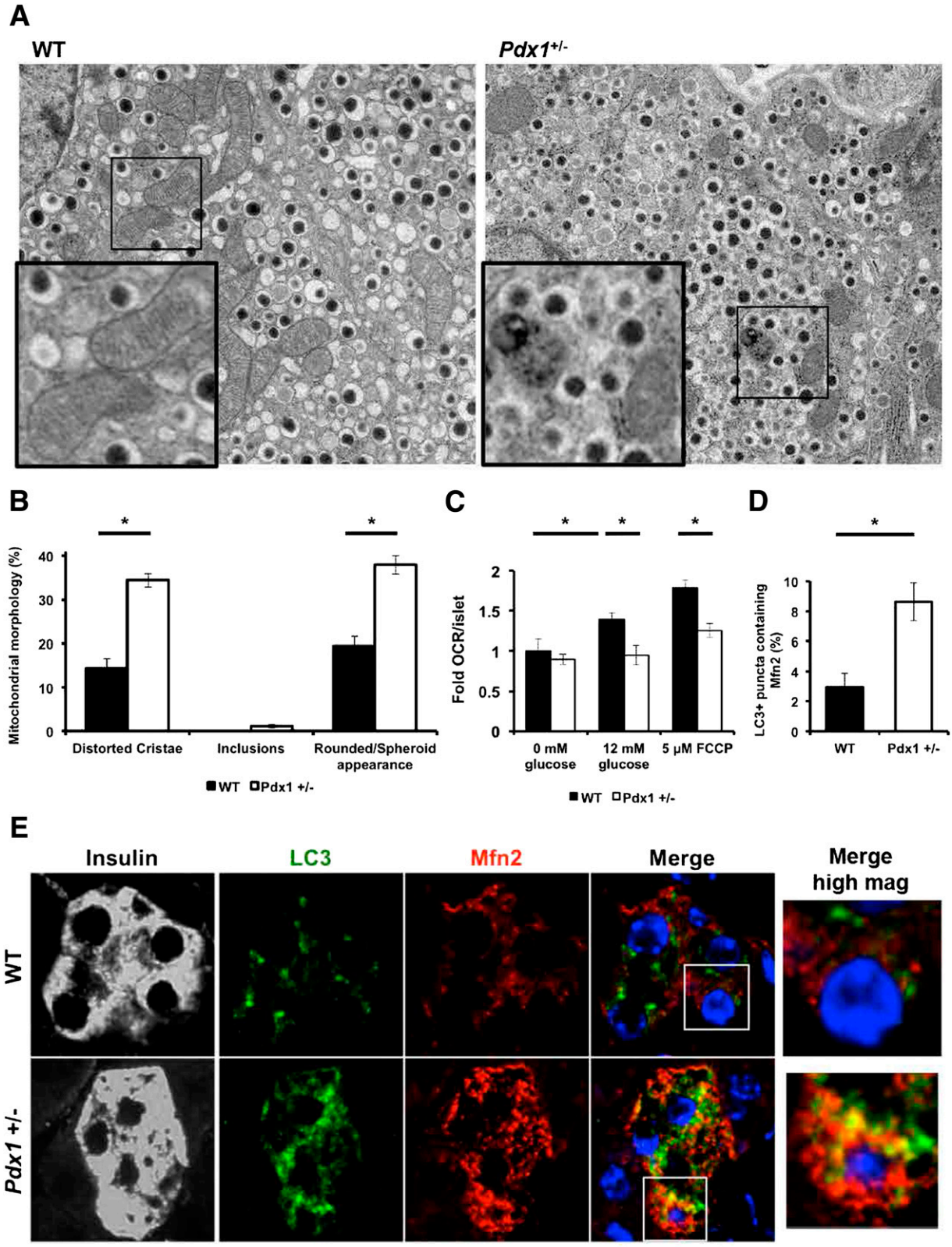

Figure 1—Pdx1 regulates mitophagy in pancreatic β-cells. *A*: Transmission EM images from 5-month-old WT and *Pdx1*$^{+/-}$ β-cells. Inset: Focused area of mitochondria on EM images. *B*: Quantification of mitochondrial morphology (% of total mitochondria) observed in WT and *Pdx1*$^{+/-}$ β-cells in transmission EM images (~250 independent mitochondria scored/animal). *n* = 3 animals/genotype. *C*: Relative oxygen consumption rate (OCR) measured in isolated WT and *Pdx1*$^{+/-}$ islets (*n* = 3/group) of 6- to 8-week-old mice. *D*: LC3/Mfn2 colocalization in LC3+ puncta quantified from 5-month-old WT and *Pdx1*$^{+/-}$ β-cells. *E*: Representative confocal image of 5-month-old WT and *Pdx1*$^{+/-}$ β-cells stained for insulin (gray), DAPI (DNA [blue]), LC3 (autophagosomes [green]), and Mfn2 (mitochondria [red]). Data are expressed as mean ± SEM. *n* = 5 mice/group and ~80 β-cells (>1,100 total LC3+ and Mfn2+ structures) were analyzed per animal. *$P < 0.05$.

RNA RT-PCR and Quantitative PCR of cDNA, Mitochondrial DNA, and Nuclear DNA

Total RNA was DNase treated (DNA-Free; Ambion) and reverse transcribed (ABI High Capacity Reverse Transcriptase kit; ABI) following the manufacturers' protocols. Fluorescence-based real-time PCR was performed using the IQ Sybr Green Supermix kit (BioRad) and the IQ-5 Single Color Real-Time PCR Detection System (BioRad). Primers were designed and optimized as previously described (9). Primer sequences for mRNA targets included Nrdp1 forward 5′-AGTGGTGATGGCCTGTGAGAA-3′ and Nrdp1 reverse 5′-CCTCCACACCATGCGCAAATA-3′. Primer sequences for Pdx1, Clec16a, and hypoxanthine guanine phosphoribosyl transferase mRNA (HPRT) were previously published (7,8). Relative gene expression normalized to hypoxanthine guanine phosphoribosyl transferase. Relative mtDNA content by quantitative (q)PCR was conducted as previously described (16) after DNA isolation with the Blood/Tissue DNeasy kit (Qiagen) according to the manufacturer's protocols.

Western Blot Analysis

Whole cell lysates (in radioimmunoprecipitation assay buffer) were generated by sonication followed by centrifugation to remove insoluble material. Lysates were resolved on 4–12% gradient Bis-Tris gels (Invitrogen) and transferred to nitrocellulose membranes as previously described (17). Primary antisera were anti-Flag (M2; Sigma), anti-Nrdp1 (Santa Cruz Biotechnology), anti-Pdx1 (253) (10), and anti–cyclophilin B (Affinity Bioreagents). Secondary antisera incubation and signal detection were performed as previously described (17). Densitometry was calculated using National Institutes of Health ImageJ software (http://imagej.nih.gov/ij/).

Viral Transductions and Transfections

Retroviral plasmids (pBABE-puro-Dest-Clec16a-Flag and pBABEpuro-LC3-GFP) were transfected into Plat-E cells using Lipofectamine 2000 transfection reagent (Invitrogen). Plasmids used for transfections included pBABE-puro-Dest-Clec16a-Flag (8) and pBABEpuro-LC3-GFP (Addgene plasmid 22405 from the laboratory of Dr. Jayanta Debnath).

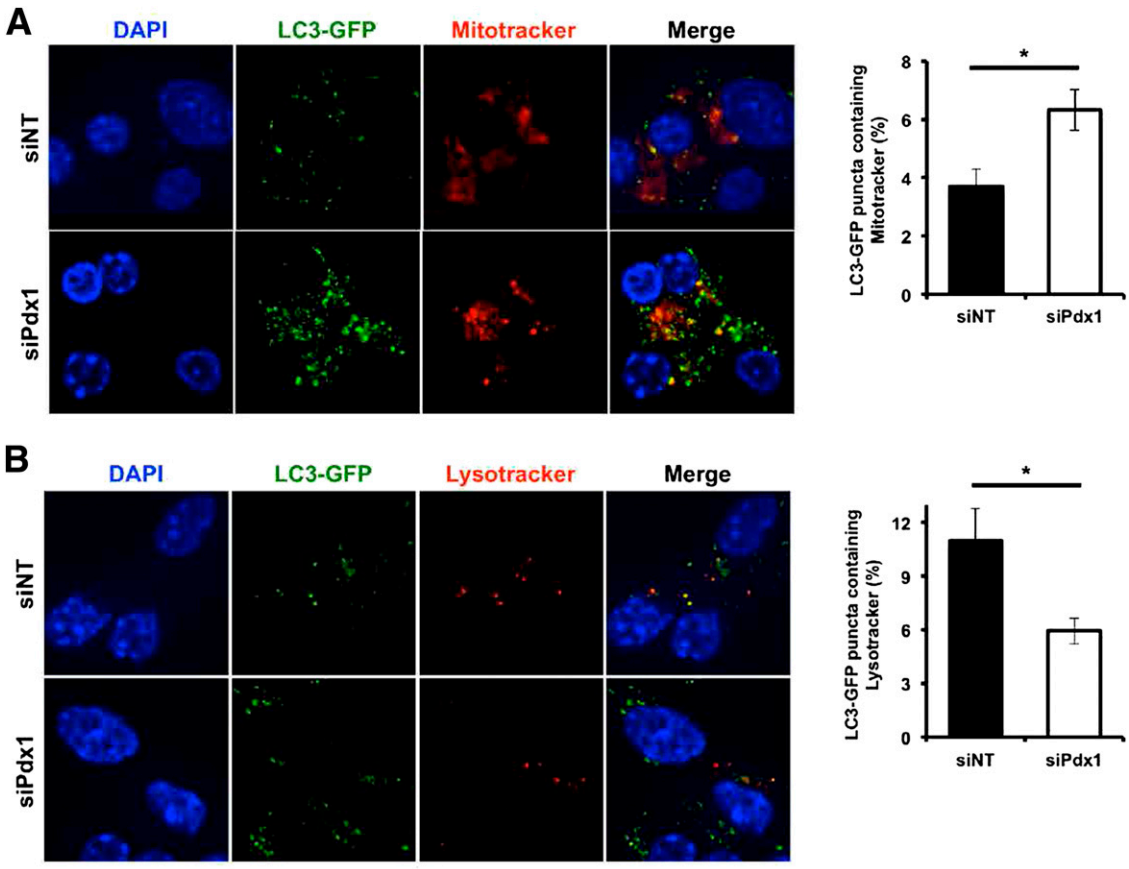

Figure 2—Pdx1 loss of function leads to impaired autophagosomal-lysosomal clearance of mitochondria in Min6 β-cells. *A*: Left, representative confocal microscopy image of si-nontargeting (siNT)- or siPdx1-treated LC3-GFP (green)–expressing Min6 β-cells after treatment with Mitotracker (red). Nuclei demarcated by DAPI (blue). Right, quantification of LC3-GFP+ puncta colocalization with Mitotracker in siNT- or siPdx1-treated LC3-GFP–expressing Min6 β-cells. *B*: Left, representative confocal microscopy image of siNT- or siPdx1-treated LC3-GFP (green)–expressing Min6 β-cells after treatment with Lysotracker (red). Nuclei demarcated by DAPI (blue). Right, quantification of LC3-GFP+ puncta colocalization with Lysotracker in siNT- or siPdx1-treated LC3-GFP–expressing Min6 β-cells. Data are expressed as mean ± SEM of three independent experiments. Approximately 80–120 cells (>1,400 total LC3-GFP+, Mitotracker+, and Lysotracker+ structures) quantified per experiment. *$P < 0.05$.

Forty-eight hours after transfection, cell supernatant was removed and filtered before placement on target cells (Min6) for transduction. Polybrene (8 μg/mL; Sigma) supplementation was added to retroviral media during infection of target cells. Selection of transduced cells was performed with Puromycin (Millipore). Transient transfection of Min6 cells was performed using an Amaxa Nucleofector as previously described (8). One nanomole of SMARTpool mouse Pdx1 and nontargeting small interfering (si)RNA was used for transient loss of function studies (Dharmacon). Nontargeting and Pdx1 siRNA sequences were published previously (18).

Statistics

Data are presented as means ± SEM, and error bars denote SEM. Statistical comparisons were performed using two-tailed Student *t* test or two-way ANOVA (Prism GraphPad). A P value <0.05 was considered significant.

RESULTS

To elucidate the mechanism(s) by which Pdx1 regulates mitochondrial function, we studied Pdx1 heterozygous mice ($Pdx1^{+/-}$), which develop glucose intolerance and reduced GSIS due to reduced mitochondrial function (6). We evaluated mitochondrial ultrastructure by transmission electron microscopy in wild-type (WT) and $Pdx1^{+/-}$ islets. $Pdx1^{+/-}$ β-cells displayed an increased number of rounded mitochondria with disordered cristae and amorphous structure (Fig. 1*A* and *B*). Dysmorphic mitochondria were not observed by EM in non–β islet cells of $Pdx1^{+/-}$ mice (data not shown). As expected, $Pdx1^{+/-}$ mice exhibited glucose intolerance (data not shown) as well as reduced glucose-stimulated and maximal oxygen consumption [after treatment with the uncoupler carbonyl cyanide 4-(trifluoromethoxy)phenylhydrazone] in isolated islets (Fig. 1*C*), suggesting that Pdx1-dependent regulation of mitochondrial structure and function could contribute to impaired glucose control in $Pdx1^{+/-}$ mice.

Structural and functional defects in mitochondria are often observed after impairments in mitophagy (19,20). Mitophagy is activated after mitochondrial damage or depolarization, leading to recruitment of autophagosomal proteins to traffic unhealthy mitochondria into autophagosomes and, ultimately, lysosomes for degradation (21). Interestingly, reduced mitochondrial membrane potential has been observed in Pdx1-deficient β-cells (22). We observed significantly increased numbers of mitochondria in autophagosomes of $Pdx1^{+/-}$ β-cells, as shown by increased colocalization of the mitochondrial outer membrane protein mitofusin 2 (Mfn2) with the autophagosome marker LC3 (Fig. 1*D* and *E*). The total number of $LC3^{+}$ puncta was also increased in $Pdx1^{+/-}$ β-cells as well as siPdx1-treated Min6 β-cells, suggesting an accumulation in autophagosomes, which is consistent with previous observations (23); however, this did not reach statistical significance (data not shown). Further, we observed an increase in mitochondria (stained with Mitotracker) targeted to LC3-GFP–labeled autophagosomes in siPdx1-treated Min6 β-cells (Fig. 2*A*). An increase in LC3-labeled mitochondria could be secondary to impaired autophagosome-lysosome fusion or to increased flux through mitophagy. To determine the cause of increased LC3-labeled mitochondria, we evaluated autophagosome-lysosome fusion in Min6 β-cells after siPdx1 treatment (or nontargeting siRNA controls). Pdx1 loss of function led to a reduced colocalization of LC3-GFP with the lysosome-specific Lysotracker dye (Fig. 2*B*), suggesting that Pdx1 deficiency impairs autophagosome-lysosome fusion. The evidence of increased mitochondrial targeting to autophagosomes along with reduced autophagosome-lysosome fusion induced by Pdx1 deficiency identifies Pdx1 as a novel regulator of mitophagy in pancreatic β-cells.

To identify the mechanistic basis for impaired mitophagy after Pdx1 loss of function, we used previously performed high-throughput expression profiling and chromatin occupancy analyses of Pdx1 in pancreatic islets (7,18). We performed a post hoc analysis of mitochondrial and autophagy-related targets of Pdx1 by overlapping cDNA expression microarray data from WT and $Pdx1^{+/-}$ islets with mitochondrial targets from the MitoCarta database (11), supplemented with ~50 additional autophagy/mitophagy related targets. Of nearly 900 transcripts analyzed, we found 4 differentially expressed transcripts with significant modulation of expression by Pdx1: Clec16a, as well as the complex I subunit Ndufs2, the aggregation suppressor Hspb7, and the NADP-dependent short-chain carbonyl reductase enzyme Dhrs4 (Table 1).

Clec16a is a recently identified gene associated with T1D in humans, with diabetogenic single nucleotide polymorphisms associated with reduced β-cell function and glucose control (8). We previously observed that Clec16a interacts with Nrdp1 and protects it from proteosomal degradation, thereby maintaining autophagosome-lysosome fusion during mitophagy. Similar to the effects of Pdx1

Table 1—Mitochondrial and autophagy-focused post hoc analysis of islet cDNA expression microarrays from WT and $Pdx1^{+/-}$ mice

Name	Description	FC ($Pdx1^{+/-}$/$Pdx1^{+/+}$)	FDR
Ndufs2	NADH dehydrogenase (ubiquinone) Fe-S protein 2	−1.769	5.48
Hspb7	Heat shock protein family, member 7 (cardiovascular)	−1.744	0
Dhrs4	Dehydrogenase/reductase (SDR family) member 4	−1.602	6.33
Clec16a	C-type lectin domain family 16, member A; KIAA0350	−1.583	6.33

Targets with fold change below −1.500 or above 1.500 and FDR below 20% are shown. FC, fold change (log2 adjusted).

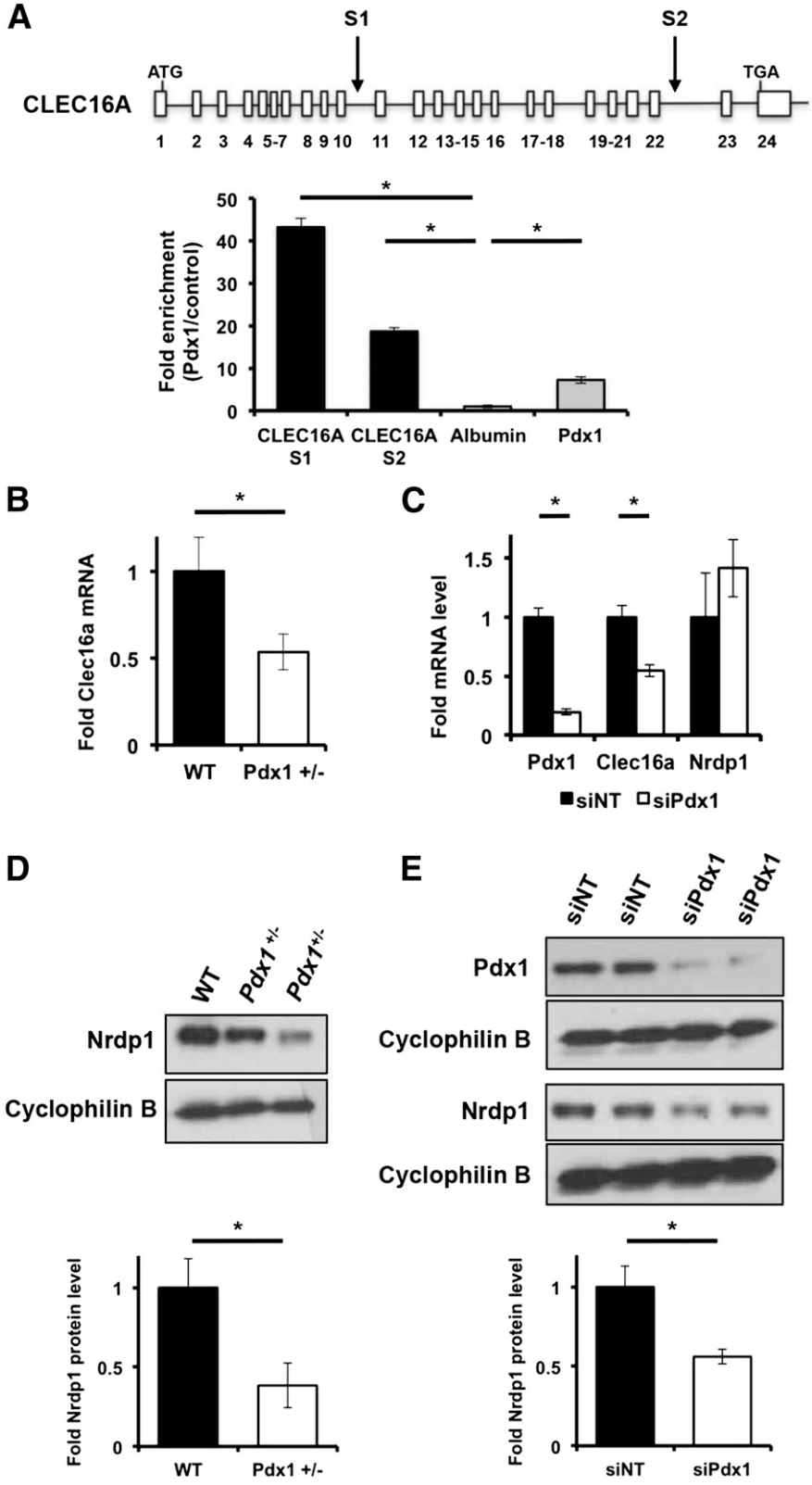

Figure 3—Pdx1 controls expression of the Clec16a-Nrdp1 pathway. *A*: Top, schematic representation of the *Clec16a* locus. Arrows delineate the two putative Pdx1 binding sites (S1 and S2). Bottom, quantitative ChIP analysis in human islets of three independent human islet donors, expressed as fold enrichment (αPdx1 vs. input control) relative to albumin occupancy. Primers designed to amplify a known Pdx1 autoregulatory binding region (45) and albumin were used as positive and negative controls, respectively. *B*: Clec16a expression by qRT-PCR of RNA isolated from 3-month-old WT and *Pdx1*$^{+/-}$ islets (n = 5–7/group). *C*: qRT-PCR of Clec16a, Pdx1, and Nrdp1 from RNA isolated from Min6 β-cells treated with si-nontargeting (siNT) or Pdx1-specific (siPdx1) siRNA (n = 3/group). *D*: Nrdp1 protein expression by Western blot of 2-month-old WT and *Pdx1*$^{+/-}$ islets (n = 3/group). *E*: Nrdp1 protein expression by Western blot in siNT- or siPdx1-treated

deficiency, loss of Clec16a expression in pancreatic islets leads to impaired mitochondrial function, insulin secretion, and glucose homeostasis, underscoring the importance of Clec16a-regulated mitophagy to pancreatic β-cell function (8). To determine whether Pdx1 regulates expression of Clec16a, we analyzed Pdx1 occupancy of the *Clec16a* locus by ChIP studies in human islets. We observed two putative Pdx1 binding sites with features of transcriptional enhancers based on previously reported high-throughput ChIP-sequencing studies (18,24). We verified Pdx1 occupancy of these sites in human islets (Fig. 3*A*) and also observed reduced Clec16a RNA expression in *Pdx1*$^{+/-}$ islets and siPdx1-treated Min6 β-cells (Fig. 3*B* and *C*). To determine whether loss of Pdx1 affects downstream targets of Clec16a, we measured Nrdp1 protein expression and observed reduced Nrdp1 expression in both *Pdx1*$^{+/-}$ islets and siPdx1-treated Min6 β-cells (Fig. 3*D* and *E*). Nrdp1 mRNA expression was not impaired in siPdx1-treated Min6 β-cells (Fig. 3*C*), consistent with a post-transcriptional effect on Nrdp1 protein expression and with our previous observation that Clec16a regulates Nrdp1 degradation. Taken together, these studies indicate that Pdx1 directly modulates expression of the Clec16a-Nrdp1 pathway in pancreatic islets.

To establish that Clec16a mediates the effect of Pdx1 on mitophagy, we studied the effect of Pdx1 loss of function on mitophagy in Min6 β-cells stably overexpressing Clec16a. Overexpression of Clec16a rescued Nrdp1 protein expression after Pdx1 siRNA treatment, suggesting that Pdx1 affects Nrdp1 expression in a Clec16a-dependent manner (Fig. 4*A* and *B*). We next evaluated mitochondrial trafficking and found that restoration of Clec16a expression significantly reduced mitochondrial colocalization with autophagosomes (Fig. 4*C*) and increased colocalization of autophagosome and lysosome markers (Fig. 4*D*) in Pdx1-deficient Min6 β-cells. Overexpression of Clec16a also improved defects in mitochondrial respiration and GSIS caused by Pdx1 deficiency (Fig. 5*A* and *B*), suggesting that Pdx1 control of mitochondrial metabolism and GSIS is mediated at least in part by its regulation of Clec16a.

Pdx1 was previously demonstrated to regulate mitochondrial DNA (mtDNA) copy number in β-cells after expression of a dominant-negative form of Pdx1 (25). We also observed a reduction in mtDNA content in *Pdx1*$^{+/-}$ islets (Fig. 5*C*). Clec16a overexpression in Min6 β-cells, however, did not restore mtDNA content after Pdx1 deficiency (Fig. 5*D*), indicating that Clec16a mediates Pdx1 regulation of mitophagy but not mtDNA copy number in β-cells.

DISCUSSION

Here, we describe Pdx1 as a transcriptional regulator of mitophagy in pancreatic β-cells. Pdx1 deficiency leads to impaired mitochondrial ultrastructure, reduced mitochondrial function, and impaired GSIS. We identify *Clec16a*, a T1D gene and regulator of mitophagy, as a downstream target of Pdx1. We find that Pdx1 occupies the *Clec16a* locus and regulates expression of Clec16a to control downstream effects on the E3 ubiquitin ligase Nrdp1 and, thus, autophagosome-lysosome fusion during mitophagy. We demonstrate that the Pdx1-Clec16a-Nrdp1 pathway is a novel regulator of β-cell mitochondrial function and insulin release.

Pdx1 has previously been implicated in the regulation of autophagy as well as mitochondrial function in β-cells (6,23,25); however, direct transcriptional targets of Pdx1 in the regulation of mitophagy had not been described. While Pdx1 loss of function has previously been shown to increase expression of Nix (also known as Bnip3l) (26), a regulator of mitophagy in erythroid cells (27), we did not observe increased expression of Nix in *Pdx1*$^{+/-}$ islets. (See Supplementary Table 1.) The other transcriptional targets we identified, Ndufs2, Hspb7, and Dhrs4, have not been implicated in the regulation of mitophagy, likely not explaining the role of Pdx1 in mitophagy that we observe. Mutations in Ndufs2, a complex I subunit protein, have been reported in patients with Leigh syndrome, a heritable mitochondrial disease resulting in cardiac and neurologic defects as well as reduced life span (28,29). Loss of Ndufs2 commonly leads to destabilization and reduced expression of complex I as well as reduced mitochondrial respiration (30,31). The small heat shock protein Hspb7 has been associated with several forms of cardiomyopathies and heart failure (32,33). Hspb7 has been reported to play a role as a suppressor of aggregated toxic polyglutamine-containing proteins, which are linked to neurodegenerative diseases and could lead to impaired mitochondrial function and apoptosis if impaired (34). Dhrs2 (Hep27) is a mitochondrial NADP-dependent short-chain dehydrogenase/reductase protein, which can regulate mitochondrial-nucleus signaling through effects on the Mdm2-p53 pathway (35). It will be of interest in the future to define the role of these genes in mitochondrial mass and function of β-cells.

Beyond its direct control of the mitochondria, Pdx1 controls several diverse functions in pancreatic β-cells that may indirectly influence mitophagy, including β-cell apoptosis, necrosis, and ER stress (7,22,26,36). Reductions in Bcl-XL and Bcl-2 expression, observed in the context of enhanced apoptosis by Pdx1 deficiency (36), induce mitophagy in HeLa cells (37). ER stress itself affects mitochondrial membrane potential and autophagy (38,39). These diverse defects observed in a Pdx1-haplosufficient β-cell potentially contribute directly and/or indirectly to an unhealthy environment ultimately leading to enhanced mitochondrial depolarization

Min6 β-cells (n = 3/group). For all Western blots, representative images chosen from among 3 independent experiments. Cyclophilin B expression serves as a loading control. Densitometry, shown adjacent to each Western blot, represents mean ± SEM of three independent experiments. qRT-PCR data expressed as mean ± SEM. *P < 0.05.

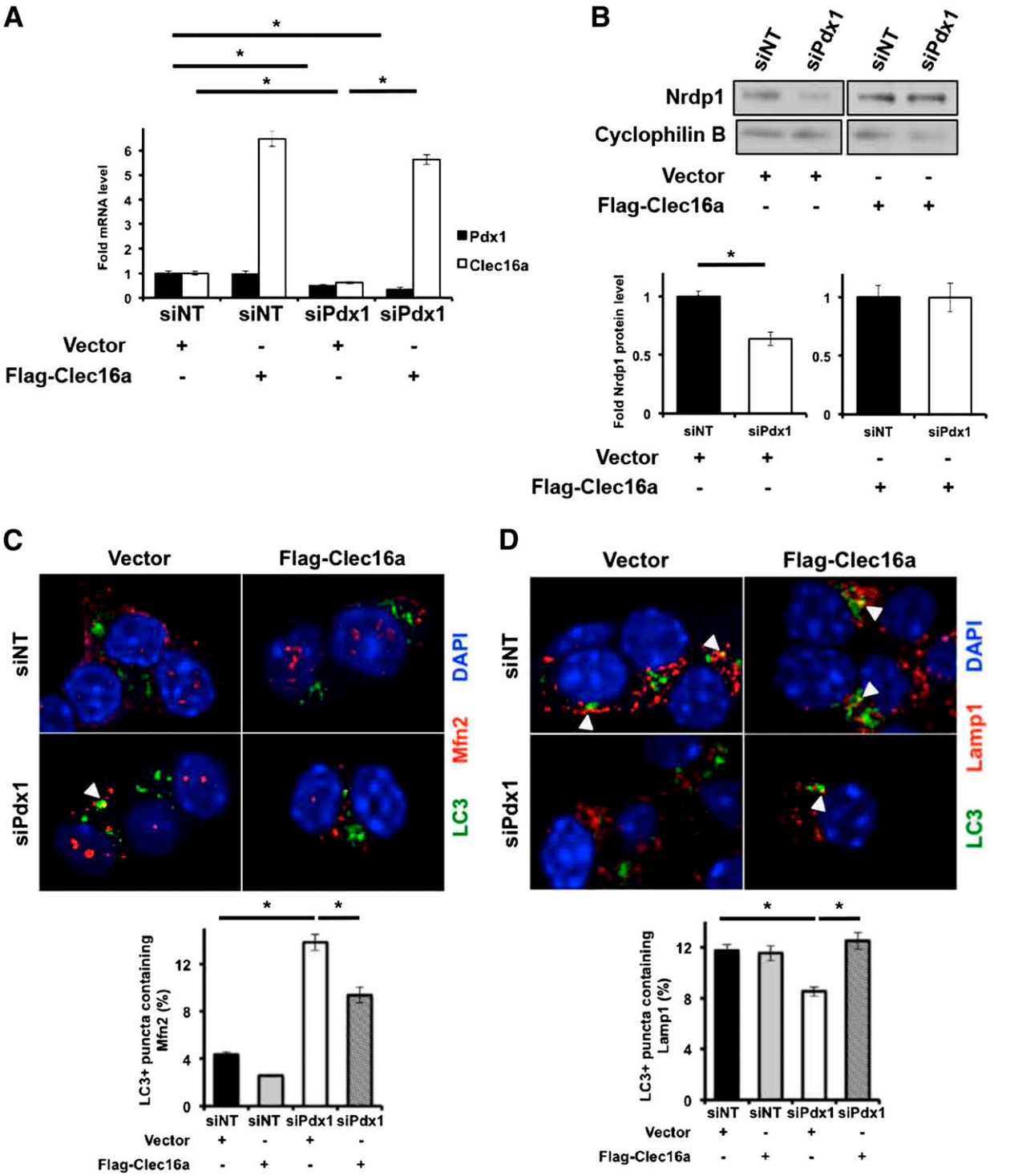

Figure 4—Restoration of Clec16a ameliorates defects in mitophagy due to Pdx1 deficiency. *A*: qRT-PCR of Clec16a and Pdx1 from RNA isolated from control or Clec16a-overexpressing Min6 β-cells treated with si-nontargeting (siNT) or Pdx1-specific (siPdx1) siRNA (n = 3/group). *B*: Representative Western blot image of Nrdp1 protein expression in siNT- or siPdx1-treated control or Clec16a-overexpressing Min6 β-cells (n = 3/group). Cyclophilin B expression serves as a loading control. Densitometry, shown adjacent to Western blot, represents mean ± SEM of 3 independent experiments. *C*: Top, representative confocal microscopy image of siNT- or siPdx1-treated control or Clec16a-overexpressing Min6 β-cells followed by staining for LC3 (green), Mfn2 (red), and DAPI (blue). Bottom, quantification of LC3+ puncta colocalization with Mfn2 in siNT- or siPdx1-treated control or Clec16a-overexpressing Min6 β-cells. Colocalized structures noted by white arrowheads. *D*: Top, representative confocal microscopy image of siNT- or siPdx1-treated control or Clec16a-overexpressing Min6 β-cells followed by staining for LC3 (green), Lamp1 (lysosomes [red]), and DAPI (blue). Colocalized structures noted by white arrowheads. Bottom, quantification of LC3+ puncta colocalization with Lamp1 in siNT- or siPdx1-treated control or Clec16a-overexpressing Min6 β-cells. Data expressed as mean ± SEM of 3 independent experiments. Approximately 80 cells (~1,200 total LC3+, Mfn2+, and Lamp1+ structures) quantified per immunofluorescence experiment. *$P < 0.05$.

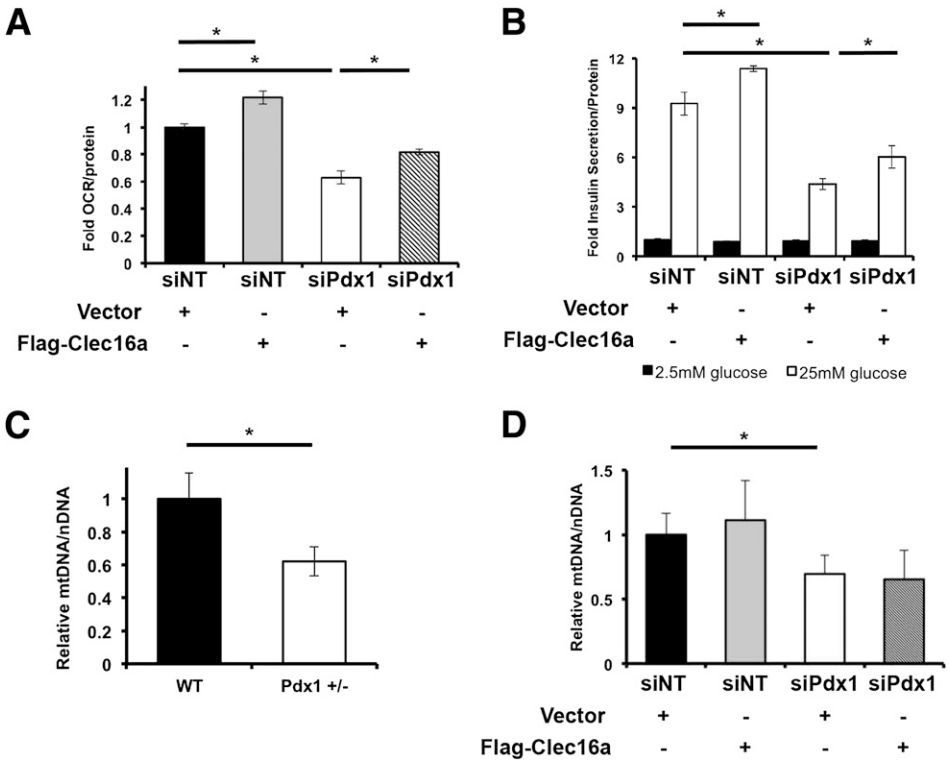

Figure 5—Overexpression of Clec16a improves mitochondrial respiration and insulin secretion but not mtDNA content after Pdx1 loss of function. *A*: Fold OCR in si-nontargeting (siNT)- or siPdx1-treated control Clec16a-overexpressing Min6 β-cells (n = 3/group). *B*: Fold insulin secretion (normalized to total protein content) in siNT- or siPdx1-treated control or Clec16a-overexpressing Min6 β-cells (n = 3/group). *C*: Relative mtDNA content measured by qPCR (normalized to nuclear DNA expression) in isolated WT and *Pdx1*$^{+/-}$ islets of 6-week-old mice (n = 4/group). *D*: Relative mtDNA content measured by qPCR (normalized to nuclear DNA expression) from DNA isolated from siNT- or siPdx1-treated control or Clec16a-overexpressing Min6 β-cells (n = 4/group). *$P < 0.05$.

and, consequently, a greater requirement for mitophagic clearance of unhealthy mitochondria. Impaired β-cell function is a common feature of both T1D and T2D, with impaired GSIS as the first observed sign of both disease processes (40,41). Both Pdx1 and Clec16a have been implicated in the regulation of GSIS in β-cells (6,8), and reduced Pdx1 expression has been observed both in the islets of prediabetic (nonobese diabetic) NOD mice, a model of T1D, and in islets from T2D donors, which could lead to dysregulation of the Clec16a-Nrdp1 pathway (42,43). Mitochondrial structural and functional defects have previously been reported in human islets from T2D donors and are characteristic of dysfunctional mitophagy (44); however, further study is needed to determine whether impaired mitophagy mediated by the Pdx1-Clec16a-Nrdp1 pathway occurs in the pathogenesis of T2D. Thus, the connection of T1D and T2D genes and pathways through a common mechanism provides a framework for developing Pdx1- and Clec16a-targeted translational therapies that may be useful for treatment of β-cell mitochondrial failure in all forms of diabetes.

Acknowledgments. The authors acknowledge N. Doliba and Q. Wei of the Penn Islet Cell Biology Core of the University of Pennsylvania Diabetes Research Center (DRC) (P30DK19525) for assistance with islet oxygen consumption studies, C. Wright and R. MacDonald for providing mouse models, and D. Williams of the Penn EM Resource Laboratory for imaging assistance. The authors thank M. Lazar, M. Birnbaum, and J. Baur, from the University of Pennsylvania, for helpful advice.

Funding. The authors acknowledge funding support from the Margaret Q. Landenberger Foundation, the Charles H. Humpton, Jr., Endowment, and the Brehm Family; the Central Society for Clinical and Translational Research (Early Career Development Award to S.A.S.); a pilot award (to B.A.K.) from the University of Pennsylvania DRC (National Institutes of Health grant P30DK19525); and National Institutes of Health grants (K08-DK089117 and R03-DK106304 to S.A.S., DK049210 to D.A.S., and DK089747 to J.C.R.).

Duality of Interest. No potential conflicts of interest relevant to this article were reported.

Author Contributions. S.A.S. conceived of, designed, and performed experiments; interpreted results; and drafted and reviewed the manuscript. A.M.F., D.N.G., and J.Y. designed and performed experiments and interpreted results. J.C.R. and B.A.K. designed and performed experiments, interpreted results, and reviewed the manuscript. D.A.S. conceived of and designed the studies, interpreted results, and edited and reviewed the manuscript. S.A.S. and D.A.S. are the guarantors of this work and, as such, had full access to all the data in the study and take responsibility for the integrity of the data and the accuracy of the data analysis.

References

1. Kaufman BA, Li C, Soleimanpour SA. Mitochondrial regulation of β-cell function: Maintaining the momentum for insulin release. Mol Aspects Med 2015; 42:91–104

2. Journo D, Mor A, Abeliovich H. Aup1-mediated regulation of Rtg3 during mitophagy. J Biol Chem 2009;284:35885–35895
3. Hani EH, Stoffers DA, Chèvre JC, et al. Defective mutations in the insulin promoter factor-1 (IPF-1) gene in late-onset type 2 diabetes mellitus. J Clin Invest 1999;104:R41–R48
4. Stoffers DA, Ferrer J, Clarke WL, Habener JF. Early-onset type-II diabetes mellitus (MODY4) linked to IPF1. Nat Genet 1997;17:138–139
5. Babu DA, Deering TG, Mirmira RG. A feat of metabolic proportions: Pdx1 orchestrates islet development and function in the maintenance of glucose homeostasis. Mol Genet Metab 2007;92:43–55
6. Brissova M, Shiota M, Nicholson WE, et al. Reduction in pancreatic transcription factor PDX-1 impairs glucose-stimulated insulin secretion. J Biol Chem 2002;277:11225–11232
7. Sachdeva MM, Claiborn KC, Khoo C, et al. Pdx1 (MODY4) regulates pancreatic beta cell susceptibility to ER stress. Proc Natl Acad Sci U S A 2009;106:19090–19095
8. Soleimanpour SA, Gupta A, Bakay M, et al. The diabetes susceptibility gene Clec16a regulates mitophagy. Cell 2014;157:1577–1590
9. Soleimanpour SA, Crutchlow MF, Ferrari AM, et al. Calcineurin signaling regulates human islet beta-cell survival. J Biol Chem 2010;285:40050–40059
10. Stoffers DA, Stanojevic V, Habener JF. Insulin promoter factor-1 gene mutation linked to early-onset type 2 diabetes mellitus directs expression of a dominant negative isoprotein. J Clin Invest 1998;102:232–241
11. Pagliarini DJ, Calvo SE, Chang B, et al. A mitochondrial protein compendium elucidates complex I disease biology. Cell 2008;134:112–123
12. Claiborn KC, Sachdeva MM, Cannon CE, Groff DN, Singer JD, Stoffers DA. Pcif1 modulates Pdx1 protein stability and pancreatic β cell function and survival in mice. J Clin Invest 2010;120:3713–3721
13. Bolte S, Cordelières FP. A guided tour into subcellular colocalization analysis in light microscopy. J Microsc 2006;224:213–232
14. Klionsky DJ, Abdalla FC, Abeliovich H, et al. Guidelines for the use and interpretation of assays for monitoring autophagy. Autophagy 2012;8:445–544
15. Khoo C, Yang J, Rajpal G, et al. Endoplasmic reticulum oxidoreductin-1-like β (ERO1lβ) regulates susceptibility to endoplasmic reticulum stress and is induced by insulin flux in β-cells. Endocrinology 2011;152:2599–2608
16. Kolesar JE, Wang CY, Taguchi YV, Chou SH, Kaufman BA. Two-dimensional intact mitochondrial DNA agarose electrophoresis reveals the structural complexity of the mammalian mitochondrial genome. Nucleic Acids Res 2013;41:e58
17. De León DD, Farzad C, Crutchlow MF, et al. Identification of transcriptional targets during pancreatic growth after partial pancreatectomy and exendin-4 treatment. Physiol Genomics 2006;24:133–143
18. Khoo C, Yang J, Weinrott SA, et al. Research resource: the pdx1 cistrome of pancreatic islets. Mol Endocrinol 2012;26:521–533
19. Ding WX, Guo F, Ni HM, et al. Parkin and mitofusins reciprocally regulate mitophagy and mitochondrial spheroid formation. J Biol Chem 2012;287:42379–42388
20. Youle RJ, Narendra DP. Mechanisms of mitophagy. Nat Rev Mol Cell Biol 2011;12:9–14
21. Jin SM, Youle RJ. PINK1- and Parkin-mediated mitophagy at a glance. J Cell Sci 2012;125:795–799
22. Fujimoto K, Chen Y, Polonsky KS, Dorn GW 2nd. Targeting cyclophilin D and the mitochondrial permeability transition enhances beta-cell survival and prevents diabetes in Pdx1 deficiency. Proc Natl Acad Sci U S A 2010;107:10214–10219
23. Fujimoto K, Hanson PT, Tran H, et al. Autophagy regulates pancreatic beta cell death in response to Pdx1 deficiency and nutrient deprivation. J Biol Chem 2009;284:27664–27673
24. Stitzel ML, Sethupathy P, Pearson DS, et al.; NISC Comparative Sequencing Program. Global epigenomic analysis of primary human pancreatic islets provides insights into type 2 diabetes susceptibility loci. Cell Metab 2010;12:443–455
25. Gauthier BR, Wiederkehr A, Baquié M, et al. PDX1 deficiency causes mitochondrial dysfunction and defective insulin secretion through TFAM suppression. Cell Metab 2009;10:110–118
26. Fujimoto K, Ford EL, Tran H, et al. Loss of Nix in Pdx1-deficient mice prevents apoptotic and necrotic β cell death and diabetes. J Clin Invest 2010;120:4031–4039
27. Zhang J, Ney PA. NIX induces mitochondrial autophagy in reticulocytes. Autophagy 2008;4:354–356
28. Loeffen J, Elpeleg O, Smeitink J, et al. Mutations in the complex I NDUFS2 gene of patients with cardiomyopathy and encephalomyopathy. Ann Neurol 2001;49:195–201
29. Tuppen HA, Hogan VE, He L, et al. The p.M292T NDUFS2 mutation causes complex I-deficient Leigh syndrome in multiple families. Brain 2010;133:2952–2963
30. Ugalde C, Janssen RJ, van den Heuvel LP, Smeitink JA, Nijtmans LG. Differences in assembly or stability of complex I and other mitochondrial OXPHOS complexes in inherited complex I deficiency. Hum Mol Genet 2004;13:659–667
31. Lazarou M, McKenzie M, Ohtake A, Thorburn DR, Ryan MT. Analysis of the assembly profiles for mitochondrial- and nuclear-DNA-encoded subunits into complex I. Mol Cell Biol 2007;27:4228–4237
32. Matkovich SJ, Van Booven DJ, Hindes A, et al. Cardiac signaling genes exhibit unexpected sequence diversity in sporadic cardiomyopathy, revealing HSPB7 polymorphisms associated with disease. J Clin Invest 2010;120:280–289
33. Stark K, Esslinger UB, Reinhard W, et al. Genetic association study identifies HSPB7 as a risk gene for idiopathic dilated cardiomyopathy. PLoS Genet 2010;6:e1001167
34. Vos MJ, Zijlstra MP, Kanon B, et al. HSPB7 is the most potent polyQ aggregation suppressor within the HSPB family of molecular chaperones. Hum Mol Genet 2010;19:4677–4693
35. Deisenroth C, Thorner AR, Enomoto T, Perou CM, Zhang Y. Mitochondrial Hep27 is a c-Myb target gene that inhibits Mdm2 and stabilizes p53. Mol Cell Biol 2010;30:3981–3993
36. Johnson JD, Ahmed NT, Luciani DS, et al. Increased islet apoptosis in Pdx1+/- mice. J Clin Invest 2003;111:1147–1160
37. Hollville E, Carroll RG, Cullen SP, Martin SJ. Bcl-2 family proteins participate in mitochondrial quality control by regulating Parkin/PINK1-dependent mitophagy. Mol Cell 2014;55:451–466
38. Senft D, Ronai ZA. UPR, autophagy, and mitochondria crosstalk underlies the ER stress response. Trends Biochem Sci 2015;40:141–148
39. Deegan S, Saveljeva S, Gorman AM, Samali A. Stress-induced self-cannibalism: on the regulation of autophagy by endoplasmic reticulum stress. Cell Mol Life Sci 2013;70:2425–2441
40. Chase HP, Cuthbertson DD, Dolan LM, et al. First-phase insulin release during the intravenous glucose tolerance test as a risk factor for type 1 diabetes. J Pediatr 2001;138:244–249
41. Defronzo RA. Banting Lecture. From the triumvirate to the ominous octet: a new paradigm for the treatment of type 2 diabetes mellitus. Diabetes 2009;58:773–795
42. Guo S, Dai C, Guo M, et al. Inactivation of specific β cell transcription factors in type 2 diabetes. J Clin Invest 2013;123:3305–3316
43. Tersey SA, Nishiki Y, Templin AT, et al. Islet β-cell endoplasmic reticulum stress precedes the onset of type 1 diabetes in the nonobese diabetic mouse model. Diabetes 2012;61:818–827
44. Anello M, Lupi R, Spampinato D, et al. Functional and morphological alterations of mitochondria in pancreatic beta cells from type 2 diabetic patients. Diabetologia 2005;48:282–289
45. Melloul D, Marshak S, Cerasi E. Regulation of pdx-1 gene expression. Diabetes 2002;51(Suppl. 3):S320–S325